









RESEARCH ARTICLE

Can axial loading restore in vivo disc geometry, opening pressure, and T2 relaxation time?

Harrah R. Newman¹  | Axel C. Moore¹  | Kyle D. Meadows¹  |
Rachel L. Hilliard²  | Madeline S. Boyes²  | Edward J. Vresilovic¹  |
Thomas P. Schaefer²  | Dawn M. Elliott¹ 

¹Department of Biomedical Engineering,
University of Delaware, Newark,
Delaware, USA

²Department of Clinical Studies, New Bolton
Center, School of Veterinary Medicine,
University of Pennsylvania, Philadelphia,
Pennsylvania, USA

Correspondence

Dawn M. Elliott, Biomedical Engineering,
University of Delaware, STAR Campus,
540 S. College Avenue, Room 201B, Newark,
DE 19713, USA.

Email: delliott@udel.edu

Funding information

National Institute of General Medical Sciences
COBRE, Grant/Award Number: P20/
GM139760; National Institute of Arthritis and
Musculoskeletal and Skin Diseases,
Grant/Award Numbers: F31/AR081687, R01/
AR050052

Abstract

Background: Cadaveric intervertebral discs are often studied for a variety of research questions, and outcomes are interpreted in the in vivo context. Unfortunately, the cadaveric disc does not inherently represent the LIVE condition, such that the disc structure (geometry), composition (T2 relaxation time), and mechanical function (opening pressure, OP) measured in the cadaver do not necessarily represent the in vivo disc.

Methods: We conducted serial evaluations in the Yucatan minipig of disc geometry, T2 relaxation time, and OP to quantify the changes that occur with progressive dissection and used axial loading to restore the in vivo condition.

Results: We found no difference in any parameter from LIVE to TORSO; thus, within 2 h of sacrifice, the TORSO disc can represent the LIVE condition. With serial dissection and sample preparation the disc height increased (SEGMENT height 18% higher than TORSO), OP decreased (POTTED was 67% lower than TORSO), and T2 time was unchanged. With axial loading, an imposed stress of 0.20–0.33 MPa returned the disc to in vivo, LIVE disc geometry and OP, although T2 time was decreased. There was a linear correlation between applied stress and OP, and this was conserved across multiple studies and species.

Conclusion: To restore the LIVE disc state in human studies or other animal models, we recommend measuring the OP/stress relationship and using this relationship to select the applied stress necessary to recover the in vivo condition.

KEYWORDS

axial load, cadaver, MRI, preload, pressure

1 | INTRODUCTION

Experiments using cadaveric intervertebral disc SEGMENTS are frequently interpreted in the context of in vivo disc function for research related to back pain, degeneration, surgery, implants, computational

models, engineered discs, and mechanobiology.^{1–3} However, there are substantial differences in the loading conditions between the LIVE, in vivo spine and excised motion SEGMENTS (bone-disc-bone). These differences can alter disc size, shape, hydration, pressure, residual stress, and mechanical behavior.⁴ Many studies have evaluated disc structure

This is an open access article under the terms of the [Creative Commons Attribution-NonCommercial](https://creativecommons.org/licenses/by-nc/4.0/) License, which permits use, distribution and reproduction in any medium, provided the original work is properly cited and is not used for commercial purposes.

© 2024 The Authors. *JOR Spine* published by Wiley Periodicals LLC on behalf of Orthopaedic Research Society.

and mechanical behavior in healthy and pathological discs through imaging, mechanical testing, and finite element modeling.^{1,2,4-13} These tools are essential for quantifying healthy disc mechanics, evaluating the changes that occur with injury or degeneration, and pre-clinical testing of repair and replacement devices. The outcomes of such studies influence clinical practice; therefore, it is imperative to quantify the differences between in vivo and cadaveric conditions, and ideally, identify methods for replicating the in vivo disc state.

To mimic the LIVE condition, many studies impose an axial preload (LOAD) that is either based on an estimation of in vivo loading or nucleus pressure.^{2,4,6,14-29} However, the target preload and nucleus pressures imposed across studies are highly variable. Prior work has found that axial preloading stiffens the disc, changes the size of the neutral zone, and reduces the range of motion.^{2,14,30,31} For human segment testing, nucleus pressurization (preloads) vary from 0 to 2.3 MPa (0–4400 N) and the preload is held for anywhere from a few minutes to the full duration of mechanical testing (sometimes called a follower load).^{15-17,24,26-30,32} Some preloads are based on previously made in vivo measures,^{22,33} while other studies do not impose a preload or provide rationale. The inconsistency, driven by a lack of evidence for chosen targets, makes it difficult to translate the results to the LIVE, in vivo state.

The disc reference state is defined by geometry, composition, and the internal/external loading of the disc immediately preceding experimental evaluations. The experimental reference state varies across studies, and it is difficult to evaluate whether the experimental reference state is representative of the LIVE disc state. Major contributors to the LIVE disc state are the surrounding structures: bones, muscles, tendons, and ligaments, which are often reduced or removed in excised specimens, substantially altering the disc loading environment and therefore the disc reference state. Previous studies have shown how sequential dissection of these elements alters the biomechanics of the spine.^{34,35} Ideally, the disc reference state in an experiment should mimic the LIVE disc. However, evaluating the LIVE disc is often difficult or impractical; fortunately, magnetic resonance imaging (MRI) can be used to repeatedly and non-invasively assess disc structure and composition, while disc opening pressure (OP) can be measured with minimally invasive techniques. Evaluating the in vivo reference state parameters of structure, composition, and pressure will enable the field to better translate ex vivo, experimental study outcomes to the LIVE condition; thus, improving clinical interpretation.

The structural, compositional, and functional differences that arise between the LIVE and excised disc conditions have not been sufficiently quantified under a consistent framework, limiting our ability to interpret cadaveric study outcomes in the context of the in vivo disc. MRI can provide non-invasive, serial evaluation of disc structure and T2 relaxation time and disc OP can be evaluated to collectively assess the changes that arise from dissection, sample preparation and applied loading conditions.^{22,33,36-39} The purpose of this work was to quantify the progressive disc geometry (structure), MRI T2 relaxation time (composition), and nucleus pressure changes (mechanical function) in the intervertebral disc from LIVE to excised bone-disc-bone SEGMENTS. To detect when changes occur, we conducted sequential isolation and reduction processes. We made comparisons with

repeated measures for specific pairs of conditions, such as between LIVE and TORSO. The results of this work will inform methods for replicating the LIVE reference condition in experimental studies.

2 | METHODS

14 Yucatan minipigs (7 male, 7 female) ~18 months old, weighing 50–90 kg, were used. The animals came from the terminal timepoint of another unrelated study with approval by the University of Delaware IACUC. The minipigs had 15 thoracic and 6 lumbar vertebrae. The anatomic descriptions for humans and quadrupeds differ, herein it was assumed that anterior is ventral and posterior is dorsal. The geometry, T2 time, and pressurization changes throughout specimen dissection and preparation were evaluated with magnetic resonance imaging (MRI) and disc opening pressures (OP).

2.1 | MRI

2.1.1 | Specimen conditions

Dissection processing

Four conditions were assessed to quantify the changes that occur with sample dissection; see Table 1 for sample sizes and levels evaluated. First, the LIVE, anesthetized animal was imaged, followed by imaging the fresh cadaver TORSO within 2 h of sacrifice (both at body temperature ~37–39°C). The next state for imaging was the intact lumbar SPINE with surrounding musculature and ligaments intact, and lastly, individual bone-disc-bone motion SEGMENT with minimal surrounding tissue and intact facets were imaged (both at room temperature ~20°C). All MRI was conducted within normal MRI specific absorption rate limits.

Specimen preparation and loading conditions

Additional conditions were used to understand the changes that occur with sample preparation and applied loading conditions (Table 2); these conditions were imposed on $n = 6$ L3-L4 discs. The methods used mimic the preparation and pre-loading process many researchers use to prepare spine segments for mechanical testing.^{4,6,19,28,30,40-42} First, the superior and inferior vertebrae of dissected SEGMENT were POTTED in polymethylmethacrylate (PMMA) bone cement. The POTTED segments were stored and imaged in a supine position, such that the weight of the potting material would not be imposed on the disc. Next, axial LOAD was applied and the segment was allowed to equilibrate under load in a phosphate-buffered saline (PBS) bath for 18 h. The LOAD was applied to achieve a nominal axial stress of 0.22 ± 0.11 MPa (mean \pm stdev), which is within the range of intradiscal pressure previously measured in supine human and bovine lumbar discs.^{18,43,44} After assessing the LOAD condition, the load was removed, and the segments were allowed to free swell in a PBS bath for 18 h before the SWELL condition was measured. Lastly, the loading was repeated, LOAD 2, and segments were equilibrated in a PBS bath for another 18 h.

TABLE 1 Specimen states assessed with MRI for changes with dissection. Comparisons denotes where repeated measures were performed between pairs of conditions, with sample sizes as shown.

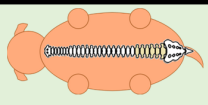
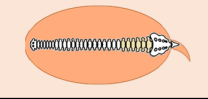
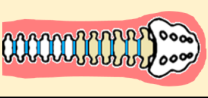

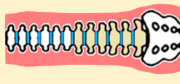
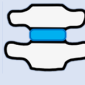
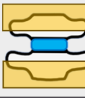



Condition	Schematic	Details	Comparisons LIVE and TORSO 4 pigs x 8 levels = 32 discs (T14-S1) TORSO and SPINE 6 pigs x 8 levels = 48 discs (T14-S1) SPINE and SEGMENT 8 pigs x 3 levels = 24 discs (L1-L2, L3-L4, L5-L6)
LIVE		Animal under anesthesia	
TORSO		Whole animal torso within 2 hours of sacrifice	
SPINE		Intact, excised spine from mid-thoracic to sacrum	
SEGMENT		Vertebrae-disc-vertebrae motion segments	

TABLE 2 Specimen states assessed for changes with specimen preparation and loading conditions in the L3-L4 disc (6 pigs x 1 level = 6 discs).

Condition	Schematic	Details
SPINE		Intact, excised spine from mid-thoracic to sacrum
SEGMENT		Vertebrae-disc-vertebrae motion segments
POTTED		Bone ends potted in PMMA bone cement
LOAD		Segment with load imposed and in PBS bath for 18 hours
SWELL		Segment supine in PBS bath for 18 hours
LOAD 2		Segment with load imposed and in PBS bath for 18 hours

Note: All evaluations were done with matched pairs across the listed conditions.

2.1.2 | Disc geometry acquisition, analysis, and statistics

A 3T Siemens Prisma MRI scanner was utilized for all scans. First, a T1-weighted FLASH (Fast Low Angle Shot) scan was used to evaluate disc geometry. Scan details are provided in Table 3. The field of view, number of slices and slice thickness were varied across conditions because the whole animal and intact spine required a larger imaging profile than the individual segments. For the LIVE, TORSO, and SPINE conditions the MRI table spine coil was used and for the subsequent SEGMENT conditions the specimens' physical size and quantity of surrounding tissue were substantially reduced, therefore flex coils were

used to improve signal return. To ensure consistent evaluation between conditions, all T1 FLASH images were sub-sampled to $0.1 \times 0.1 \times 0.5 \text{ mm}^3$ with Convert3D,⁴⁵ allowing for consistent selection of the mid-sagittal slice and identification of disc boundaries.

The T1-weighted FLASH images were used to assess disc geometry. From the mid-sagittal slice, a custom Matlab script was used to trace the disc boundary to determine the sagittal disc area and a line was drawn anterior-posterior to determine the sagittal disc width (Figure 1A).^{36,46} The disc height (H_{Disc}) was calculated as the nucleus mid-sagittal area (A_{Nuc}) divided by the nucleus anterior-posterior width (W_{Nuc}) (Figure 1B).

TABLE 3 MRI scan sequence parameters including repetition time (TR) and echo time (TE).

Scan	Output	Slices	In-plane resolution (mm)	Slice thickness (mm)	TR (ms)	TE (ms)
T1 FLASH	Geometry	16–42	0.43–0.55	1–3	9.6	3.7
T2 CPMG	T2 relax time	1	0.39–0.68	2–5	3000	13.6, 27.2, ... 340

Note: The number of slices and slice thickness depended on the size of the specimen, where larger specimens (LIVE/TORSO/SPINE) had more slices and larger slice thickness and smaller specimens (SEGMENT and subsequent conditions) had fewer slices and smaller slice thickness, within the ranges noted.

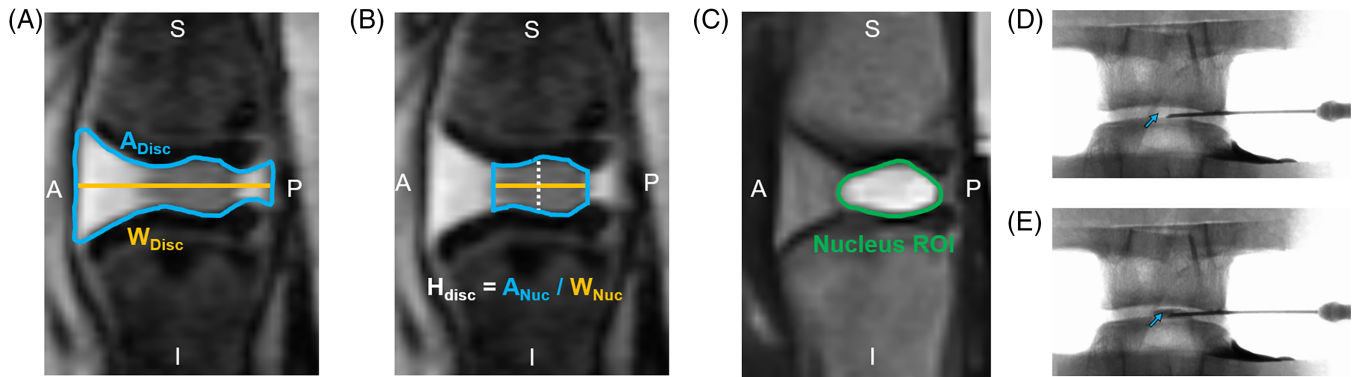


FIGURE 1 (A) On the FLASH MRI, the disc boundary was outlined for assessing disc area and an anterior–posterior line was drawn to assess disc width. (B) The disc height was calculated as the nucleus area divided by the nucleus width as shown. (C) From the T2 MRI, the T2 relaxation time was calculated for the nucleus region. (D) Using fluoroscopic guidance, the OP was measured by inserting a needle into the nucleus and increasing the pressure until (E) the radiopaque contrast agent was visualized in the disc nucleus.

$$H_{\text{Disc}} = \frac{A_{\text{Nuc}}}{W_{\text{Nuc}}} \quad (1)$$

Additionally, the axial disc area (see Equation (3) in Opening Pressure Methods) was used to calculate the nominal stress in the LOAD cases as the applied load divided by the axial cross sectional disc area (CSA_{Disc}):

$$\sigma = \frac{\text{Load}}{CSA_{\text{Disc}}} \quad (2)$$

Data were displayed with box and whisker plots, where the center line is the median, colored box boundaries are the 25% and 75% quantiles, and the whiskers extend to 1.5 times the interquartile range unless this exceeds the data range, in which case the whiskers end at the maximum/minimum data value. Statistical analysis was conducted with repeated, matched pair Students *t*-tests and Bonferroni correction. Post hoc power analyses were performed to confirm that the sample sizes achieved a power of at least 0.9.

2.1.3 | T2 relaxation time acquisition, analysis, and statistics

A T2-weighted CPMG (Carr-Purcell Meiboom-Gill) scan was taken for assessing the T2 relaxation time in the disc nucleus (Table 3). Prior studies indicate that T2 time is correlated with tissue water content/disc hydration^{37,47–53} and proteoglycan content.^{48–53} Some work also suggests associations with collagen content,^{37,48,53,54} collagen

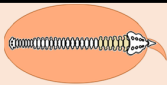
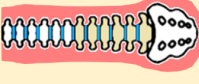
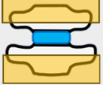


alignment,^{37,54} and matrix organization.³⁷ T2 relaxation time was calculated from the intensity decay in the nucleus region of interest (Figure 1C) using a noise-corrected exponential decay function, in accordance with our prior work.^{36,53} Statistical analysis was conducted with paired Students *t*-tests and Bonferroni correction.

2.2 | Opening pressure

2.2.1 | Specimen conditions

In addition to the MRI measurements of geometry and T2 time, the OP of the disc was assessed in a separate cohort of samples; see Table 4 for sample sizes and levels evaluated. The OP was not measured on every sample in every condition. The OP was first measured in the TORSO, via a posterior incision through the skin and muscle. The spine was then excised to measure the OP of the intact SPINE, followed by dissection of individual motion segments which were POTTED in PMMA as previously described. After OP was evaluated in the POTTED segments, they were placed in a PBS bath with an applied axial stress that ranged between 0 and 0.74 MPa. Following 18 h of loaded equilibration, the LOAD OP measurement was performed. The load was then removed for an immediate subsequent measure of the UNLOAD OP. At the POTTED segment and subsequent conditions, a mixture of segments with intact facets and removed facets were used. Facetectomy alters the range of motion and can greatly impact torsion capacity, but it is least impactful for axial creep loading and only has meaningful effects at high loads.^{2,4,16} Given the low loads

TABLE 4 Specimen states evaluated for disc opening pressure.

Condition	Schematic	Details	Specimens
TORSO		Whole animal or torso within 2 hours of sacrifice	10 discs
SPINE		Intact, excised spine from mid-thoracic to sacrum	15 discs
POTTED		Bone ends potted in PMMA bone cement	14 discs
LOAD		Segment with a load between 0.11-0.74 MPa imposed in PBS bath for 18 hours	15 discs
UNLOAD		Segment immediately after load removed	14 discs

Note: For each condition, the levels assessed were randomized such that two animals were evaluated for 10–15 discs between T12–L5 per condition. Every disc was not measured at every condition. All comparisons were done with unpaired groups across the listed conditions.

imposed, we assume that facetectomy will not have a significant effect on OP.

$$CSA_{Disc} = W_{DiscCor} \times W_{DiscSag} \times \frac{\pi}{4} \quad (3)$$

2.2.2 | Acquisition, analysis, and statistics

An IntelliSystem 25 (Merit Medical) syringe fitted with a 22G beveled needle was used for contrast injection while the pressure was measured with the IntelliSystem Inflation System Monitor (Merit Medical). Fluoroscopy (Orthoscan) was used to guide the needle insertion (Figure 1D) and visually monitor for the contrast penetration (Figure 1E). The radio-opaque contrast agent, Omnipaque at 300 mg/mL, was pressurized and once the syringe pressure matched and exceeded the internal disc pressure, contrast would enter the disc space. Once contrast was visualized, the injection was stopped, and pressure recorded.

Multiple punctures were performed on the same disc, which could affect the OP measurement. Previous work found no permanent changes in disc mechanics or height if the needle diameter was less than 25% of the disc height, as the disc is described as having a self-sealing effect.^{24,55–57} In the present study the needle diameter (0.72 mm, 22G needle) was 24.6% of the disc height across all conditions; therefore, we did not anticipate the needle puncture to influence OP measures. We checked this by comparing OP for multiple punctures on the same disc.

Fluoroscopic images were used to estimate the axial cross-sectional area of the disc (CSA_{Disc}). A reference standard was included and used to scale each image. The coronal and sagittal width of the superior and inferior endplates were measured using ImageJ. The average coronal ($W_{DiscCor}$) and sagittal ($W_{DiscSag}$) width were used to estimate the CSA_{Disc} based on the assumption of an ellipse as follows:

The nominal axial stress on the disc for the LOAD case was then calculated as the applied load divided by cross sectional area, (Equation (2)).

The OP changes between the TORSO, SPINE, POTTED segment, and UNLOAD segment were compared with unpaired Student's *t*-tests and Bonferroni correction between conditions. The LOAD segment was not compared with the other conditions as a range of loads were used. The LOAD segment OP was used to establish a linear relationship between the nominal applied load and the resultant disc OP.

3 | RESULTS

3.1 | MRI

3.1.1 | Disc geometry

Effect of dissection

The effect of dissection on disc geometry, progressing from the live animal to a single segment (Table 1), was assessed. We first assessed whether the disc geometry in the TORSO within 2 h of sacrifice was the same as in the LIVE spine using a paired *t*-test ($n = 32$ discs/group). There were no significant differences in mid-sagittal disc height, anterior–posterior width, or area between the LIVE and TORSO conditions (Figure 2). These measurements were all highly correlated between conditions ($m \approx 1$, $R^2 \approx 1$, $p < 0.001$, Figure 3A–C). Therefore, the TORSO within 2 h of sacrifice can be considered to represent the LIVE condition.

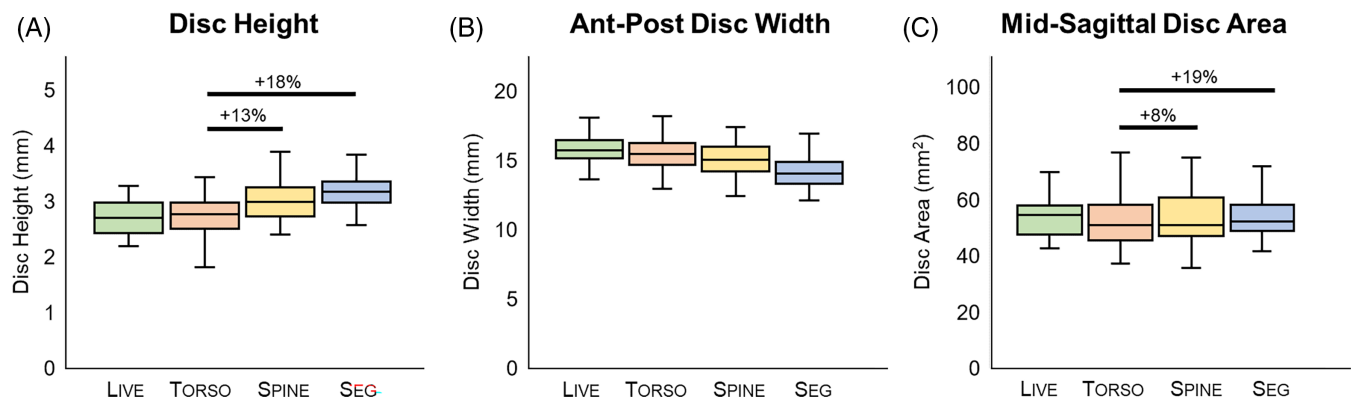


FIGURE 2 Mid-sagittal disc geometry assessed with MRI throughout the dissection process from the Live animal down to individual motion segments. (A) Disc height and (C) area significantly increased from the Torso to the Spine and Segment conditions while (B) disc width was not significantly changed between any conditions. See Table 1 for sample sizes; outcomes significant if $p < 0.05$.

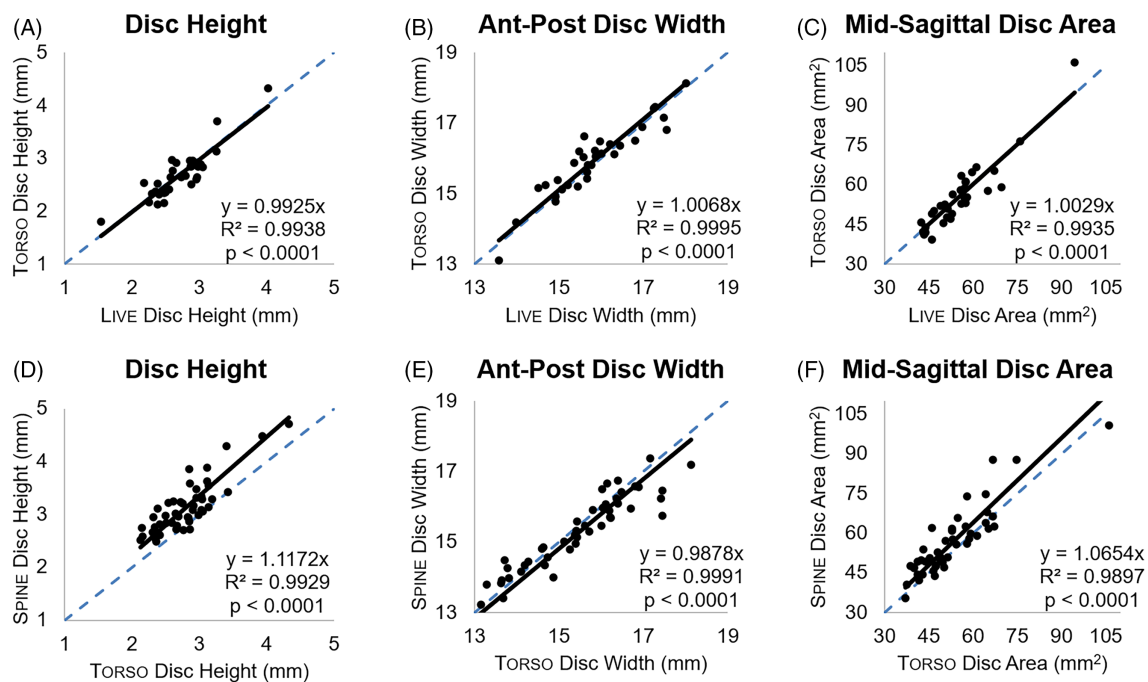


FIGURE 3 Correlations between the Live and Torso conditions for (A) disc height, (B) disc width, and (C) disc area. All parameters were significantly correlated with slopes of nearly one, there is no significant difference in disc geometry between the Live and Torso conditions (paired t -test, Figure 2). Correlations between the Torso and Spine conditions for (D) disc height, (E) disc width, and (F) disc area found all parameters were significantly correlated. See Table 1 for sample sizes.

The spine is regularly subjected to loads from surrounding tissue, but with dissection many of these surrounding structures are reduced or removed which alters the load imposed on the disc. While there were no significant changes between the LIVE and Torso conditions, extracting the intact SPINE from the Torso caused significant changes in the disc geometry (Figure 2, Figure 3D–F). From the Torso to SPINE conditions, the mid-sagittal disc height and area increased, though the anterior–posterior width did not significantly change (Figure 2). The same trends continued when the SPINE was dissected down to individual SEGMENT, further increasing disc height and area, with trending decreases in disc width (Figure 2). Generally, with dissection the

discs increased in mid-sagittal height and area while the anterior–posterior width was maintained.

Effect of specimen preparation and loading conditions

The L3–L4 segment was assessed in a series of specimen preparation and loading conditions, including the intact SPINE, isolated SEGMENT, POTTED segment, LOAD segment, free SWELL segment, and repeated LOAD 2 segment (Table 2). From the SPINE to SEGMENT conditions there were no significant geometry changes (Figure 4). This is consistent with the dissection comparisons above, which included L1–L2 and L4–L5, in addition to L3–L4 (Figure 2). The mid-sagittal disc height

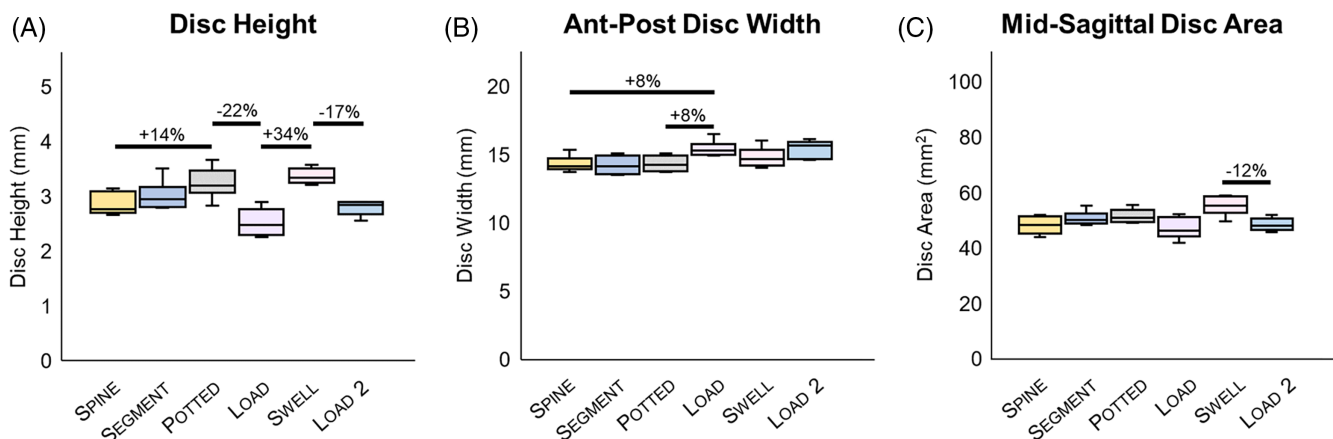


FIGURE 4 Mid-sagittal disc geometry with specimen preparation and loading conditions for $n = 6L3-L4$ discs. (A) Disc height increased from the spine to potted condition. Both loading conditions decreased the disc height and free swelling increased the disc height. (B) Disc width was significantly increased with the first loading case only. (C) Disc area decreased with the second loading but was otherwise unchanged. Outcomes significant if $p < 0.05$.

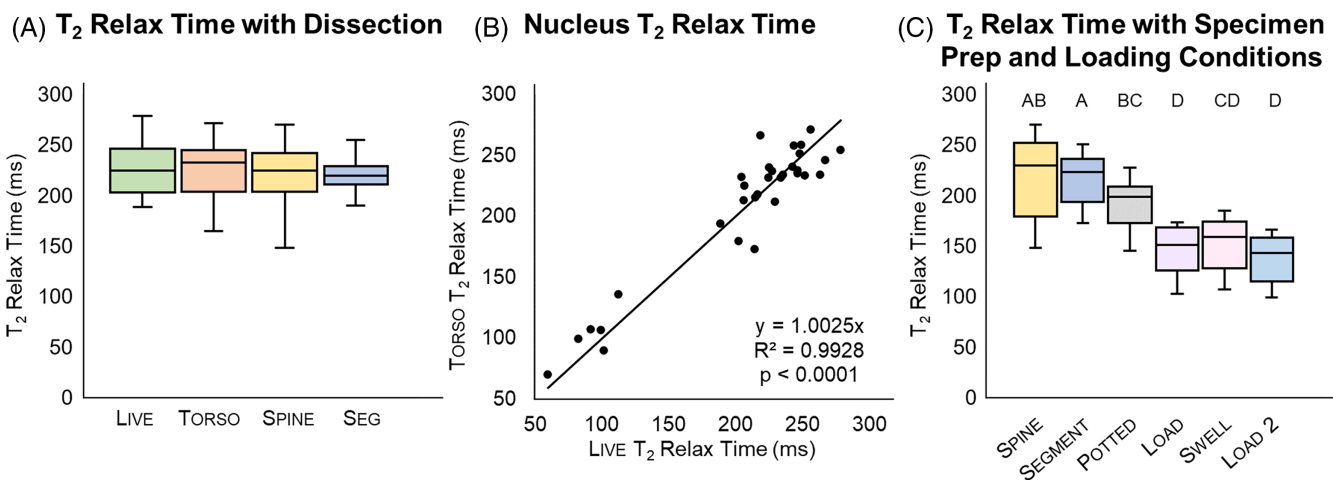


FIGURE 5 (A) T2 relaxation time did not significantly change through the dissection process from Live animal to individual motion Segments (see Table 1 for sample sizes). (B) The T2 time in the Live and Torso conditions were highly well correlated ($n = 32$ discs). (C) T2 time generally decreased from the Segment to Potted to Loaded conditions, and then remained unchanged between the first Load, free Swell, and second Load conditions (see Table 2 for sample sizes). Any groups that do not share a letter are significantly different ($p < 0.05$) from each other.

increased by 14% in the POTTED condition compared to the SPINE condition, whereas mid-sagittal disc area and width remained unchanged (Figure 4). Following potting, the LOAD segment was compressed with 0.22 ± 0.11 MPa stress, which reduced disc height by 22% and increased disc width by 8% compared to the POTTED condition, with no significant change in disc area (Figure 4). After the first 18 h loading cycle, the disc was allowed to free SWELL which recovered the mid-sagittal height, width, and area such that they were not significantly different from the initial SEGMENT or POTTED conditions (Figure 4). Finally, when reloaded in the LOAD 2 condition, the segment again exhibited decreased mid-sagittal disc height and area, compared to the preceding free SWELL segment (Figure 4). The LOAD and LOAD 2 conditions were not significantly different from each other. In

summary, specimen preparation and loading conditions mostly impacted mid-sagittal disc height with small changes in the disc width and area.

3.1.2 | Nucleus T₂ relaxation time

Effect of dissection

In addition to disc geometry, we also sought to evaluate the T2 relaxation time of the nucleus pulposus, as the T2 time is known to strongly correlate with disc water^{37,47–53} and proteoglycan content.^{48–53} The T2 time did not change throughout the dissection process from LIVE to TORSO to SPINE down to individual SEGMENT conditions ($p > 0.05$,

Figure 5A). Furthermore, the T2 time in the LIVE and TORSO conditions were highly correlated ($R^2 \sim 1$, $p < 0.001$) with a linear fit slope of nearly 1 (Figure 5B), indicating that the TORSO spine closely represents the LIVE spine for evaluating T2 times.

Effect of specimen preparation and loading conditions

Comparing the experimental preparation conditions, the L3-L4 segments did not exhibit significant T2 time changes from the SPINE to SEGMENT conditions (Figure 5C), similar to the L1-L2 and L4-L5 results from the dissection conditions (Figure 5A). However, compared to SEGMENT, T2 decreased by 12% in the POTTED condition and decreased another 24% in the LOAD condition (Figure 5C). There was negligible further change in the SWELL and LOAD 2 conditions. Overall, the T2 time reduced with specimen processing and, unlike geometry, remained low throughout subsequent loading and swelling conditions.

3.2 | Disc opening pressure

Primarily, we sought to evaluate whether the disc OP is altered with sequential dissection and the relationship between axial stress and OP. Due to the loss of restraining structures and soft tissue preload, we expected OP to decrease at each step. We found that OP decreased from the TORSO to SPINE to POTTED segment conditions as expected (Figure 6A). The intrinsic OP (POTTED, 0 MPa applied stress) was 0.11 ± 0.06 MPa.

Following the POTTED condition, the disc was loaded for 18 h in a bath (LOAD). The applied axial stress (LOAD), ranged from 0 to 0.74 MPa, exhibited a linear relationship with OP ($R^2 = 0.87$, $p < 0.0001$) with a slope of 1.11 and intercept of 0.082 MPa (Figure 6B). The UNLOAD disc OP was not significantly different from the POTTED disc OP (Figure 6A), indicating that the effect of loading is recoverable and happens over short time scales.

From the LOAD OP/Stress relationship, we can estimate the imposed stress that would be required to achieve a particular OP. Given this relationship and the known TORSO OP (0.38 ± 0.08 MPa), we can back-calculate the axial stress required to achieve the measured in vivo OP from the fit line (Figure 6B). OP/Stress relationship from Figure 6B:

$$OP = 1.112 * (\text{Applied stress}) + 0.082 \quad (4)$$

Rearranging to solve for the applied stress:

$$\text{Applied stress} = \frac{OP - 0.082}{1.112} \quad (5)$$

Therefore, evaluating Equation (5) for the known TORSO OP, we found that an applied stress of 0.27 ± 0.07 MPa should recover in vivo disc pressurization.

There was no significant change in OP with repeated punctures (Figure 7A). Additionally, the presence or absence of intact facets did

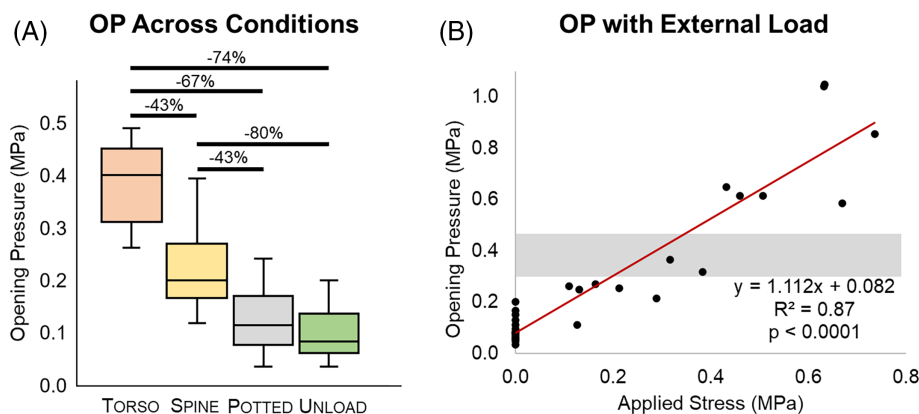


FIGURE 6 (A) Disc opening pressure measurements across conditions ($n = 10-15/\text{group}$). The Loaded case was excluded from this statistical assessment as the segments underwent a range of load magnitudes. (B) For the Loaded cases, the applied stress was highly correlated with the measured disc opening pressure. The gray area marks the opening pressure measured in the Torsio condition for reference. Outcomes significant if $p < 0.05$.

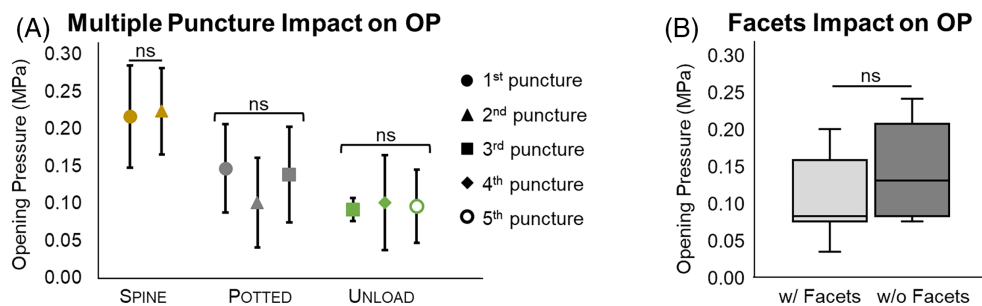


FIGURE 7 (A) Repeated needle punctures did not alter OP measured ($n = 3-18/\text{group}$), unpaired t -test between the number of punctures within each condition found $p > 0.3$ for all conditions. (B) Potted segments with or without facets did not yield a different intrinsic OP, unpaired t -test $p > 0.3$ ($n = 7/\text{group}$).

not significantly impact the disc OP at the imposed stresses evaluated (Figure 7B).

4 | DISCUSSION

This study provided serial evaluation of the geometry, T2 relaxation time, and opening pressure (OP) of the disc to assess the changes that occur with dissection that should be recovered in order to evaluate the disc mechanics with reference to the LIVE condition. The study provides evidence that the cadaver TORSO, within 2 h of sacrifice, can be used to represent the LIVE condition and that with dissection, the OP, and thus axial load, generally decreases. Moreover, specific imposed loading conditions can recover disc geometry and OP to match in vivo measures, but T2 time does not recover. Combining all outcomes, disc geometry and disc OP were optimally recovered with an axial stress of 0.20–0.33 MPa.

4.1 | Live and cadaver conditions not different

The disc geometry and T2 times in the LIVE and fresh cadaveric TORSO were the same, all measures were highly correlated with slopes of nearly one. This is a particularly valuable result as it demonstrates that for future large animal work, at the terminal time point, the animal can be sacrificed within 2 h prior to imaging. Cadaveric imaging eliminates the need for veterinary anesthesia, reduces the number of critical personnel required and improves imaging feasibility at terminal time points in large animal imaging studies.

4.2 | Effect of dissection

Throughout the dissection process, surrounding tissues are removed that impose axial restraints on the disc. From the intact TORSO to excised SPINE (which is the state in which human cadavers for research are generally provided) the spine is separated from the limbs and adjacent organs; then from the SPINE condition to the individual SEGMENTS, the surrounding musculature, tendons, and ligaments are resected. The removal of surrounding tissue structures resulted in progressive reduction of OP (Figure 6A) and the increased disc height seen from the TORSO to SPINE to SEGMENT conditions (Figure 2A), which collectively support the expected trend of decreased axial load with surrounding tissue reduction.

Despite significant changes in the disc geometry and OP with dissection, the T2 time was not significantly different throughout the dissection conditions (Figure 5A). While there have been many studies evaluating the factors affecting T2 relaxation time, including water content,^{37,47–53} macromolecule and matrix content and organization,^{37,48–54} the lack of change indicates that, the factors within the NP which determine T2 relaxation time were not significantly altered. Moreover, this lack of change suggests that PBS-soaked gauze was sufficient to maintain external hydration for the SEGMENT conditions.

4.3 | Effect of specimen preparation and loading conditions

The 0.22 ± 0.11 MPa applied stress in the LOAD and LOAD 2 conditions successfully recovered disc geometry to within the ranges measured for the LIVE and TORSO conditions (Figure 4A). The OP increased linearly with the magnitude of the stress imposed, further detailed below (Figure 6B). Importantly, the change in OP under the conditions studied appeared to be exclusively due to hydrostatic and elastic stress. This is supported by the linear OP/stress relationship and by the UNLOAD segment instantaneously returning the disc to the POTTED segment pressure (Figure 6A). Given that the OP is highly dependent on the axial load, once the spine or segment is removed from the body, if not compressed, the disc pressure and geometry no longer effectively mimic the in vivo disc.

We anticipated the free SWELL condition would enable fluid-uptake by the disc and induce substantial increases in disc geometry parameters. The disc nucleus is densely populated by proteoglycans which are responsible for maintaining the disc fluid content. In the absence of external loads, the disc was able to expand axially, and we found that the disc height increased following the free SWELL. Interestingly, the disc width remained unchanged. The disc was free to expand laterally, but was likely limited by attachment to the adjacent vertebral bodies and the fibrous annulus. The disc sagittal area was trending toward an increase compared to the LOAD segment, likely driven by the increased disc height and maintained disc width.

4.4 | T2 time effects

The POTTED T2 time was not significantly different from the SPINE T2 time; thus, fluid motion in the disc space was likely minimal throughout the potting process, where it was necessary to handle the segment and leave it on the bench (wrapped in PBS-soaked gauze) in a vertical position while the PMMA cured.

The T2 time was substantially reduced with the first LOAD condition, presumably due to fluid exudation with the applied axial stress. After LOAD, the next condition was a free SWELL in a PBS bath, intended to allow fluid to passively enter the disc and restore disc hydration and T2 time. While the disc took in water, as supported by the increased disc height and area in the SWELL condition, surprisingly, the T2 time was not recovered as was expected. This observation leads to speculation about possible changes in water and tissue organization impacting T2 time as correlations between T2 time and water content^{37,47–53} have been previously established.

Previous MRI and benchwork has shown T2 time correlates with water^{37,47–53} and proteoglycan content,^{48–53} with some work suggesting the impact of additional factors including collagen content,^{37,48,53,54} collagen alignment,^{37,54} and matrix organization.³⁷ Therefore, the first LOAD condition may have caused structural and/or macromolecule compositional changes that impacted the T2 time and were not recoverable with disc rehydration alone. Although, we have no explanation for this result and it was not expected, the result is

likely important as it was experimentally repeatable. This finding warrants future investigation.

Despite the T2 time reduction with LOAD and subsequent conditions, the porcine T2 times evaluated are approximately two times the magnitude of those measured for healthy human disc,³⁶ such that the T2 times in the LOAD and SWELL conditions would still be considered, from a clinical perspective, to be healthy, hydrated discs.

4.5 | Imposed stress and opening pressure relationship

The relationship between imposed stress and disc OP has been assessed in other models and species, summarized in Figure 8A.^{22,29,33,58} All studies show a highly linear relationship between applied axial stress and disc OP, but with variations in slope and intercept. These variations could potentially be attributed to variations across species in disc and nucleus size,⁴⁶ composition, and presence of notochordal cells in the NP, as well as disc health³³ and methodological differences such as loading mechanism,^{18,29} method for calculating disc area,^{19,33,46} and method for assessing OP. Since human OP has been directly measured in vivo,^{22,43} the relationship between OP and axial stress is useful to choose a representative axial load in a cadaveric experiment. Unfortunately, the variation in the OP/stress relationship between studies means that population-specific OP/stress measurements are likely required for study design. If the OP/stress relationship is obtained from prior work, the closest available match of species, age, and loading mechanism should be used.

In addition to comparing the OP/stress relationship across species, we further sought to assess the correlation of the linear fit slope and intercept with the proteoglycan (GAG) and water content by species (Figure 8B,C).⁹ The GAG and water content values are taken from Beckstein+2008, a study independent of the OP/stress evaluations.

We found that the OP/stress slope had a trending correlation ($p = 0.06$) with both nucleus GAG content and water content; interestingly, the correlations were in opposing directions (Figure 8B). A higher OP/stress slope was associated with increasing GAGs, but with decreasing water content. The OP/stress intercept did not exhibit significant trends with nucleus GAG or water content ($p > 0.4$, Figure 8C). These results collectively indicate the disc responsiveness to load, indicated by the OP/stress linear fit slope, increases with higher nucleus GAG content and lower water content.

For the stress and opening pressure relationship comparisons, there were several differences between studies that should be considered: firstly, the present study was conducted in independent segments while all others were serial assessments on the same segments. For studies that provided the nominal load (N), the imposed stress was calculated as load divided by the disc area (Equation (2)). Reitmaier+2013²² conducted experiments in live animals while all other studies were conducted in cadaveric samples. Additionally, the sheep disc area was not provided in Reitmaier+2013²² and was therefore assumed from O'Connell + 2007.⁴⁶ Despite variations across studies, they all show relatively consistent trends.

4.6 | Recommendations to restore in vivo disc condition

For human cadaver experiments, the specimens arrive in the SPINE state, with the changes from LIVE to SPINE generally unknown. Importantly, this study quantified increases in disc height and area from LIVE to SPINE states, ideally these changes should be minimized by applying an axial load such that the experimental reference state closely mimics the LIVE disc state. However, replicating the LIVE disc state, may not be important for all research questions and should be considered by investigators based on their study goals.

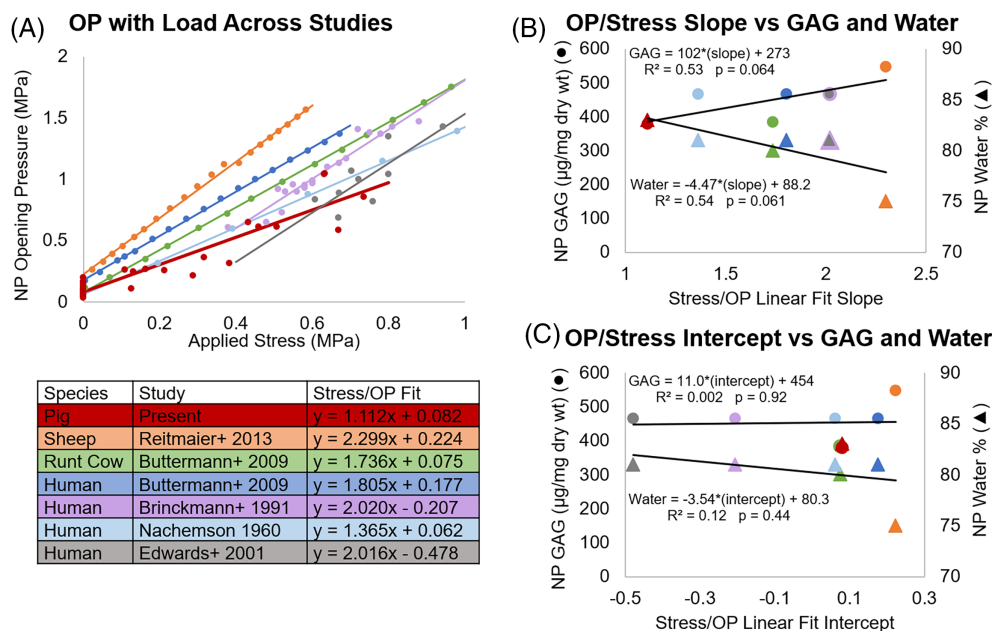


FIGURE 8 (A) Relationship between applied stress and NP opening pressure across studies and species all in the lumbar spine. (B) NP GAG and water content by species from Beckstein+ 2008 were compared to the (B) linear regression slopes and (C) linear regression intercepts for each study.

We found that allowing the segment to free swell (SWELL), then imposing an axial stress of 0.22 ± 0.11 MPa (LOAD 2) resulted in recovery of disc height and width (TORSO:LOAD height and width differences both <1%). From the imposed OP/stress relationship we found that an applied stress of 0.27 ± 0.07 MPa recovers in vivo disc pressurization. Combining all outcomes, we recommend allowing the segment to swell under load with an imposed axial stress of 0.20–0.33 MPa for optimizing the recovery of in vivo, LIVE disc geometry and OP in the minipig model. The applied stress needed will likely vary for human and other large animal species; however, prior OP studies can be used to compute the stress required to recover LIVE disc parameters.^{18,22,29,33,58} As noted above, despite loading and swelling attempts to recover disc parameters, the T2 time was not recoverable to LIVE values.

4.7 | Study limitations

This study is not without limitations. The LIVE condition was assessed under anesthesia in a supine position which minimizes active muscle forces and reduces spinal load; therefore, the live, active animal may experience greater spinal loads, multiaxial loading, and constraints from surrounding spinal structures.³⁵ The LIVE and TORSO conditions were evaluated at body temperature, while all subsequent conditions were evaluated at room temperature. The specimen temperature contributes to the osmotic pressure; however, the temperature contribution was assumed to be of significantly less magnitude than the pressure contribution from the physical load on the disc. As the TORSO OP could not be assessed through the thick porcine back, an incision was required to access the disc. However, it is likely that any loss of stress due to the incision was very small compared to that imposed by the larger structures and intact physical constraints containing the spine. Lastly, the UNLOAD condition was preceded by LOAD of varying magnitude (0.11–0.74 MPa) which could have impacted the subsequent UNLOAD OP measurement. However, regardless of the LOAD, within the evaluated range, the UNLOAD disc was equivalent to the POTTED disc.

5 | CONCLUSION

In the present study we quantified the changes in disc geometry (structure), T2 relaxation time (composition), and OP (mechanical function) to enable development of preloading protocols that establish the in vivo disc reference state prior to mechanical testing or other assessments. Intervertebral disc geometry, T2 time, and OP are altered by progressive dissection, specimen preparation, and imposed loading conditions. In cadaveric studies, it is important to mitigate these changes to ensure that specimens best represent the in vivo condition and so that study outcomes can be interpreted with respect to the live, in vivo condition. In this minipig model, an imposed axial stress of 0.20–0.33 MPa successfully recovered in vivo, LIVE disc geometry and OP. We recommend assessing the OP/stress

relationship for study specimens and using this relationship to guide the applied stress needed to recover the LIVE disc state.

AUTHOR CONTRIBUTIONS

The project concept was developed by HRN, ACM, EJ, and DME. Data collection was conducted by HRN, ACM, KDM, RLH, MSB, and TPS. Data interpretation and manuscript preparation was done by HRN, ACM, EDJ, TPS, and DME.

ACKNOWLEDGMENTS

The authors would like to thank the University of Delaware Center for Biomedical and Brain Imaging for their MRI support and Adriana Barba for veterinary assistance. This work was supported by NIH/NIAMS R01 AR050052, NIH/NIAMS F31 AR081687, and NIH/NIGMS COBRE P20 GM139760.

CONFLICT OF INTEREST STATEMENT

The authors declare no conflicts of interest.

ORCID

Harrah R. Newman  <https://orcid.org/0000-0001-5555-4308>

Axel C. Moore  <https://orcid.org/0000-0002-9469-4351>

Kyle D. Meadows  <https://orcid.org/0000-0002-1113-8633>

Rachel L. Hilliard  <https://orcid.org/0000-0002-6836-0024>

Madeline S. Boyes  <https://orcid.org/0009-0003-0386-9123>

Edward J. Vresilovic  <https://orcid.org/0000-0002-9591-8409>

Thomas P. Schaer  <https://orcid.org/0000-0002-4340-8212>

Dawn M. Elliott  <https://orcid.org/0000-0003-4792-1029>

REFERENCES

- Amin DB, Sommerfeld D, Lawless IM, Stanley RM, Ding B, Costi JJ. Effect of degeneration on the six degree of freedom mechanical properties of human lumbar spine segments. *J Orthop Res*. 2016;34(8):1399-1409. doi:10.1002/jor.23334
- Gardner-Morse MG, Stokes IA. Physiological axial compressive preloads increase motion segment stiffness, linearity and hysteresis in all six degrees of freedom for small displacements about the neutral posture. *J Orthop Res*. 2003;21(3):547-552. doi:10.1016/S0736-0266(02)00199-7
- Marini G, Studer H, Huber G, Püschel K, Ferguson SJ. Geometrical aspects of patient-specific modelling of the intervertebral disc: collagen fibre orientation and residual stress distribution. *Biomech Model Mechanobiol*. 2016;15(3):543-560. doi:10.1007/s10237-015-0709-6
- Costi JJ, Ledet EH, O'Connell GD. Spine biomechanical testing methodologies: the controversy of consensus vs scientific evidence. *JOR Spine*. 2021;4(1):1-25. doi:10.1002/jsp2.1138
- Keller T, Holm S, Hansson T, Spengler D. 1990 Volvo award in experimental studies: the dependence of intervertebral disc mechanical properties on physiologic conditions. *Spine (Phila Pa 1976)*. 1990;15(8):751-761.
- Bezi SE, Klineberg EO, O'Connell GD. Effects of axial compression and rotation angle on torsional mechanical properties of bovine caudal discs. *J Mech Behav Biomed Mater*. 2018;77:353-359. doi:10.1016/j.jmbbm.2017.09.022
- Schmidt H, Shirazi-Adl A, Galbusera F, Wilke HJ. Response analysis of the lumbar spine during regular daily activities-A finite element analysis. *J Biomech*. 2010;43(10):1849-1856. doi:10.1016/j.jbiomech.2010.03.035

8. Niemeyer F, Wilke HJ, Schmidt H. Geometry strongly influences the response of numerical models of the lumbar spine-A probabilistic finite element analysis. *J Biomech.* 2012;45(8):1414-1423. doi:[10.1016/j.jbiomech.2012.02.021](https://doi.org/10.1016/j.jbiomech.2012.02.021)
9. Beckstein JC, Sen S, Schaer TP, Vresilovic EJ, Elliott DM. Comparison of animal discs used in disc research to human lumbar disc: axial compression mechanics and glycosaminoglycan content. *Spine (Phila Pa 1976)*. 2008;33(6):166-173. doi:[10.1097/BRS.0b013e318166e001](https://doi.org/10.1097/BRS.0b013e318166e001)
10. Newman HR, DeLucca JF, Peloquin JM, Vresilovic EJ, Elliott DM. Multiaxial validation of a finite element model of the intervertebral disc with multigenerational fibers to establish residual strain. *JOR Spine.* 2021;4(2):1-16. doi:[10.1002/jsp2.1145](https://doi.org/10.1002/jsp2.1145)
11. Jacobs NT, Cortes DH, Vresilovic EJ, Elliott DM. Biaxial tension of fibrous tissue: using finite element methods to address experimental challenges arising from boundary conditions and anisotropy. *J Biomech Eng.* 2013;135(2):1-10. doi:[10.1115/1.4023503](https://doi.org/10.1115/1.4023503)
12. Cortes DH, Jacobs NT, DeLucca JF, Elliott DM. Elastic, permeability and swelling properties of human intervertebral disc tissues: a benchmark for tissue engineering. *J Biomech.* 2014;47(9):2088-2094. doi:[10.1016/j.jbiomech.2013.12.021](https://doi.org/10.1016/j.jbiomech.2013.12.021)
13. Iatridis JC, Ap GI. Mechanisms for mechanical damage in the intervertebral disc annulus fibrosus. *J Biomech.* 2004;37(8):1165-1175. doi:[10.1016/j.jbiomech.2003.12.026](https://doi.org/10.1016/j.jbiomech.2003.12.026)
14. Janevic J, Ashton-Miller JA, Schultz AB. Large compressive preloads decrease lumbar motion segment flexibility. *J Orthop Res.* 1991;9(2):228-236. doi:[10.1002/jor.1100090211](https://doi.org/10.1002/jor.1100090211)
15. Patwardhan A, Havey R, Meade K, Lee B, Dunlap B. A follower load increases the load-carrying capacity of the lumbar spine in compression. *Spine (Phila Pa 1976)*. 1999;24(10):1003-1009.
16. Mcglashen KM, Miller JAA, Schultz AB, Anderson GBJ. Load displacement behavior of the human lumbo-sacral joint. *Orthopaedic Research Society.* 1987;5:488-496.
17. Crisco JJ, Fujita L, Spenciner DB. The dynamic flexion/extension properties of the lumbar spine in vitro using a novel pendulum system. *J Biomech.* 2007;40(12):2767-2773. doi:[10.1016/j.jbiomech.2006.12.013](https://doi.org/10.1016/j.jbiomech.2006.12.013)
18. Buttermann GR, Beaubien BP, Saeger LC. Mature runt cow lumbar intradiscal pressures and motion segment biomechanics. *Spine J.* 2009;9(2):105-114.
19. Lim S, Huff RD, Veres JE, Satish D, O'Connell GD. Disc geometry measurement methods affect reported compressive mechanics by up to 65%. *JOR Spine.* 2022;5(3):1-8. doi:[10.1002/jsp2.1214](https://doi.org/10.1002/jsp2.1214)
20. Showalter BL, Beckstein JC, Martin JT, et al. Comparison of animal discs used in disc research to human lumbar disc: torsion mechanics and collagen content. *Spine (Phila Pa 1976)*. 2012;37(15):E900-E907. doi:[10.1097/BRS.0b013e31824d911c](https://doi.org/10.1097/BRS.0b013e31824d911c)
21. Vergroesen PPA, Emanuel KS, Peeters M, Kingma I, Smit TH. Are axial intervertebral disc biomechanics determined by osmosis? *J Biomech.* 2018;70:4-9. doi:[10.1016/j.jbiomech.2017.04.027](https://doi.org/10.1016/j.jbiomech.2017.04.027)
22. Reitmaier S, Schmidt H, Ihler R, et al. Preliminary investigations on intradiscal pressures during daily activities: an in vivo study using the merino sheep. *PLoS One.* 2013;8(7):1-10. doi:[10.1371/journal.pone.0069610](https://doi.org/10.1371/journal.pone.0069610)
23. Dreischarf M, Shirazi-Adl A, Arjmand N, Rohlmann A, Schmidt H. Estimation of loads on human lumbar spine: a review of in vivo and computational model studies. *J Biomech.* 2016;49(6):833-845. doi:[10.1016/j.jbiomech.2015.12.038](https://doi.org/10.1016/j.jbiomech.2015.12.038)
24. Elliott DM, Yerramalli CS, Beckstein JC, Boxberger JI, Johannessen W, Vresilovic EJ. The effect of relative needle diameter in puncture and sham injection animal models of degeneration. *Spine (Phila Pa 1976)*. 2008;33:588-596.
25. DeLucca JF, Cortes DH, Jacobs NT, Vresilovic EJ, Duncan RL, Elliott DM. Human cartilage endplate permeability varies with degeneration and intervertebral disc site. *J Biomech.* 2016;49(4):550-557. doi:[10.1016/J.JBIOMECH.2016.01.007](https://doi.org/10.1016/J.JBIOMECH.2016.01.007)
26. Amin DB, Lawless IM, Sommerfeld D, Stanley RM, Ding B, Costi JJ. The effect of six degree of freedom loading sequence on the in-vitro compressive properties of human lumbar spine segments. *J Biomech.* 2016;49(14):3407-3414. doi:[10.1016/j.jbiomech.2016.09.009](https://doi.org/10.1016/j.jbiomech.2016.09.009)
27. Costi JJ, Stokes IA, Gardner-Morse MG, Iatridis JC. Frequency-dependent behavior of the intervertebral disc in response to each of six degree of freedom dynamic loading solid phase and fluid phase contributions. *Spine (Phila Pa 1976)*. 2008;33(16):1731-1738.
28. Cripton PA, Bruehlmann SB, Orr TE, Oxland TR, Nolte L-P. In vitro axial preload application during spine flexibility testing: towards reduced apparatus-related artefacts. *J Biomech.* 2000;33:1559-1568.
29. Brinckmann P, Grootenboer H. Change of disc height, radial disc bulge, and intradiscal pressure from discectomy an in vitro investigation on human lumbar discs. *Spine (Phila Pa 1976)*. 1991;16(6):641-646.
30. Gardner-Morse MG, Stokes IAF. Structural behavior of human lumbar spinal motion segments. *J Biomech.* 2004;37(2):205-212. doi:[10.1016/j.jbiomech.2003.10.003](https://doi.org/10.1016/j.jbiomech.2003.10.003)
31. Edwards WT, Hayes WC, Posner I, White AA, Mann RW. Variation of lumbar spine stiffness with load. *J Biomech Eng.* 1987;109(1):35-42. doi:[10.1115/1.3138639](https://doi.org/10.1115/1.3138639)
32. Zirbel SA, Stolworthy DK, Howell LL, Bowden AE. Intervertebral disc degeneration alters lumbar spine segmental stiffness in all modes of loading under a compressive follower load. *Spine J.* 2013;13(9):1134-1147. doi:[10.1016/j.spinee.2013.02.010](https://doi.org/10.1016/j.spinee.2013.02.010)
33. Nachemson AL. Lumbar intradiscal pressure. Experimental studies on post-mortem material. *Acta Orthop Scand Suppl.* 1960;43:1-104. doi:[10.3109/ort.1960.31.suppl-43.01](https://doi.org/10.3109/ort.1960.31.suppl-43.01)
34. Abumi K, Panjabi MM, Kramer KM, Duranceau J, Oxland T, Crisco JJ. Biomechanical evaluation of lumbar spinal stability after graded facetectomies. *Spine (Phila Pa 1976)*. 1990;15(11):1142-1147. doi:[10.1097/00007632-199011010-00011](https://doi.org/10.1097/00007632-199011010-00011)
35. Wilke HJ, Wolf S, Claes LE, Arand M, Wiesend A. Influence of varying muscle forces on lumbar intradiscal pressure: an in vitro study. *J Biomech.* 1996;29(4):549-555. doi:[10.1016/0021-9290\(95\)00037-2](https://doi.org/10.1016/0021-9290(95)00037-2)
36. Meadows KD, Cauchy PJK, Peloquin JM, Vresilovic EJ, Newman HR, Elliott DM. MRI-based measurement of in vivo disc mechanics in a young population due to flexion, extension, and diurnal loading. *JOR Spine.* 2022;2023:1-14. doi:[10.1002/jsp2.1243](https://doi.org/10.1002/jsp2.1243)
37. Stelzeneder D, Kovács BK, Goed S, et al. Effect of short-term unloading on T2 relaxation time in the lumbar intervertebral disc—in vivo magnetic resonance imaging study at 3.0 tesla. *Spine J.* 2012;12(3):257-264. doi:[10.1016/j.spinee.2012.02.001](https://doi.org/10.1016/j.spinee.2012.02.001)
38. Cheung KMC, Karppinen J, Chan D, et al. Prevalence and pattern of lumbar magnetic resonance imaging changes in a population study of one thousand forty-three individuals. *Spine (Phila Pa 1976)*. 2009;34(9):934-940. doi:[10.1097/BRS.0b013e3181a01b3f](https://doi.org/10.1097/BRS.0b013e3181a01b3f)
39. Takatalo J, Karppinen J, Niinimäki J, et al. Prevalence of degenerative imaging findings in lumbar magnetic resonance imaging among young adults. *Spine (Phila Pa 1976)*. 2009;34(16):1716-1721. doi:[10.1097/BRS.0b013e3181ac5fec](https://doi.org/10.1097/BRS.0b013e3181ac5fec)
40. Adams MA. Spine update mechanical testing of the spine an appraisal of methodology, results, and conclusions. *Spine (Phila Pa 1976)*. 1995;20(19):2151-2156.
41. Amin DB, Lawless IM, Sommerfeld D, Stanley RM, Ding B, Costi JJ. Effect of potting technique on the measurement of six degree-of-freedom viscoelastic properties of human lumbar spine segments. *J Biomech Eng.* 2015;137(5):054501. doi:[10.1115/1.4029698](https://doi.org/10.1115/1.4029698)
42. DeLucca JF, Amin DB, Peloquin JM, Vresilovic EJ, Costi JJ, Elliott DM. Off-axis response due to mechanical coupling across all six degrees of freedom in the human disc. *JOR Spine.* 2019;2(1):e1047. doi:[10.1002/jsp2.1047](https://doi.org/10.1002/jsp2.1047)
43. Nachemson AL, Morris JM. In vivo measurements of intradiscal pressure. Discometry, a method for the determination of pressure in the lower lumbar discs. *J Bone Joint Surg Am.* 1964;46(5):1077-1092.

44. Wilke H-J, Neef P, Caimi M, Hoogland T, Claes LE. New in-vivo measurements of pressures in the intervertebral disc in daily life. *Spine (Phila Pa 1976)*. 1999;24(8):755-762.
45. Yushkevich PA, Piven J, Hazlett HC, et al. User-guided 3D active contour segmentation of anatomical structures: significantly improved efficiency and reliability. *Neuroimage*. 2006;31(3):1116-1128. doi:10.1016/j.neuroimage.2006.01.015
46. O'Connell GD, Vresilovic EJ, Elliott DM. Comparison of animals used in disc research to human lumbar disc geometry. *Spine (Phila Pa 1976)*. 2007;32(3):328-333. doi:10.1097/01.brs.0000253961.40910.c1
47. Ellingson AM, Mehta H, Polly DW, Ellermann J, Nuckley DJ. Disc degeneration assessed by quantitative T2* (T2 star) correlated with functional lumbar mechanics. *Spine (Phila Pa 1976)*. 2013;38(24):612-625. doi:10.1097/BRS.0b013e3182a59453.Disc
48. Ellingson AM, Nagel TM, Polly DP, Ellermann J, Nuckley DJ. Quantitative T2* (T2 star) relaxation times predict site specific proteoglycan content and residual mechanics of the intervertebral disc throughout degeneration. *J Ortho Res*. 2014;32(8):1083-1089.
49. Marinelli NL, Houghton VM, Anderson PA. T2 relaxation times correlated with stage of lumbar intervertebral disk degeneration and patient age. *Am J Neuroradiol*. 2010;31(7):1278-1282. doi:10.3174/ajnr.A2080
50. Martin JT, Oldweiler AB, Kosinski AS, et al. Lumbar intervertebral disc diurnal deformations and T2 and T1rho relaxation times vary by spinal level and disc region. *Eur Spine J*. 2022;31(3):746-754. doi:10.1007/s00586-021-07097-4
51. Benneker LM, Heini PF, Anderson SE, Alini M, Ito K. Correlation of radiographic and MRI parameters to morphological and biochemical assessment of intervertebral disc degeneration. *Eur Spine J*. 2005;14(1):27-35. doi:10.1007/s00586-004-0759-4
52. Antoniou J, Pike GB, Steffen T, et al. Quantitative magnetic resonance imaging in the assessment of degenerative disc disease. *Magn Reson Med*. 1998;40(6):900-907. doi:10.1002/mrm.1910400616
53. Meadows KD, Johnson CL, Peloquin JM, Spencer RG, Vresilovic EJ, Elliott DM. Impact of pulse sequence, analysis method, and signal to noise ratio on the accuracy of intervertebral disc T2 measurement. *JOR Spine*. 2020;3(3):1-12. doi:10.1002/jsp2.1102
54. Yoon M, Hong S, Kang C, Sik KA, Kim B. T1rho and T2 mapping of lumbar intervertebral disc: correlation with degeneration and morphologic changes in different disc regions. *Magn Reson Imaging*. 2016;34(7):932-939. <https://www.ptonline.com/articles/how-to-get-better-mfi-results>
55. Torre OM, Evashwick-Rogler TW, Nasser P, Iatridis JC. Biomechanical test protocols to detect minor injury effects in intervertebral discs. *J Mech Behav Biomed Mater*. 2018;2019(95):13-20. doi:10.1016/j.jmbbm.2019.03.024
56. Michalek AJ, Iatridis JC. Height and torsional stiffness are most sensitive to annular injury in large animal intervertebral discs. *Bone*. 2008;23(1):1-7.
57. Wang JL, Tsai YC, Wang YH. The leakage pathway and effect of needle gauge on degree of disc injury post anular puncture: a comparative study using aged human and adolescent porcine discs. *Spine (Phila Pa 1976)*. 2007;32(17):1809-1815. doi:10.1097/BRS.0b013e31811ec282
58. Thomas Edwards W, Ordway NR, Zheng Y, McCullen G, Han Z, Yuan HA. Peak stresses observed in the posterior lateral annulus. *Spine (Phila Pa 1976)*. 2001;26:1753-1759.

How to cite this article: Newman HR, Moore AC, Meadows KD, et al. Can axial loading restore in vivo disc geometry, opening pressure, and T2 relaxation time? *JOR Spine*. 2024;7(2):e1322. doi:10.1002/jsp2.1322